HHS Public Access

Author manuscript

Cancer Discov. Author manuscript; available in PMC 2020 May 05.

Published in final edited form as:

Cancer Discov. 2018 November ; 8(11): 1376–1389. doi:10.1158/2159-8290.CD-17-0841.

Targeting the MTF2–MDM2 Axis Sensitizes Refractory Acute Myeloid Leukemia to Chemotherapy

Harinad B. Maganti[1,2,3,*], **Hani Jrade**[1,2,4,*], **Christopher Cafariello**[1,2,4], **Janet L. Manias Rothberg**[1,2,4], **Christopher J. Porter**[5], **Julien Yockell-Lelièvre**[1,2], **Hannah L. Battaion**[1,2,4], **Safwat T. Khan**[1], **Joel P. Howard**[1], **Yuefeng Li**[1,2,4], **Adrian T. Grzybowski**[6], **Elham Sabri**[7], **Alexander J. Ruthenburg**[6], **F. Jeffrey Dilworth**[1,2,4], **Theodore J. Perkins**[1,3,5], **Mitchell Sabloff**[8,9], **Caryn Y. Ito**[1,4], **William L. Stanford**[1,2,3,4]

[1]The Sprott Center for Stem Cell Research, Regenerative Medicine Program, Ottawa Hospital Research Institute, Ottawa, Ontario, Canada.

[2]Ottawa Institute of Systems Biology, Ottawa, Ontario, Canada.

[3]Department of Biochemistry, Microbiology and Immunology, University of Ottawa, Ottawa, Ontario, Canada.

[4]Department of Cellular and Molecular Medicine, University of Ottawa, Ottawa, Ontario, Canada.

[5]Ottawa Bioinformatics Core Facility, The Sprott Center for Stem Cell Research, Ottawa Hospital Research Institute, Ottawa, Ontario, Canada.

[6]Department of Molecular Genetics and Cell Biology, The University of Chicago, Chicago, Illinois.

[7]Clinical Epidemiology Methods Centre, Ottawa Hospital Research Institute, Ottawa, Ontario, Canada.

[8]Division of Hematology, Department of Medicine, University of Ottawa, Ottawa, Ontario, Canada.

[9]Ottawa Hospital Research Institute, Ottawa, Ontario, Canada.

Abstract

Corresponding Authors: William L. Stanford, Ottawa Hospital Research Institute, 5th Floor Critical Care Wing (CCW), Room 5214, Ottawa K1H 8L6, Canada. Phone: 613-737-8899, ext. 75495; Fax: 613-739-6294; wstanford@ohri.ca; and Caryn Y. Ito, cito@ohri.ca.
*H.B. Maganti and H. Jrade contributed equally to this article.

Authors' Contributions

Conception and design: H.B. Maganti, H. Jrade, M. Sabloff, C.Y. Ito, W.L. Stanford

Development of methodology: H.B. Maganti, H. Jrade, W.L. Stanford

Acquisition of data (provided animals, acquired and managed patients, provided facilities, etc.): H.B. Maganti, H. Jrade, C. Cafariello, J.L. Manias Rothberg, J. Yockell-Lelièvre, H.L. Battaion, S.T. Khan, Y. Li, A.T. Grzybowski, A.J. Ruthenburg, M. Sabloff

Analysis and interpretation of data (e.g., statistical analysis, biostatistics, computational analysis): H.B. Maganti, H. Jrade, C.J. Porter, J. Yockell-Lelièvre, A.T. Grzybowski, E. Sabri, F.J. Dilworth, T.J. Perkins, M. Sabloff, C.Y. Ito, W.L. Stanford

Writing, review, and/or revision of the manuscript: H.B. Maganti, H. Jrade, C. Cafariello, J. Yockell-Lelièvre, H.L. Battaion, A.T. Grzybowski, T.J. Perkins, M. Sabloff, C.Y. Ito, W.L. Stanford

Administrative, technical, or material support (i.e., reporting or organizing data, constructing databases): H.B. Maganti, H. Jrade, M. Sabloff

Study supervision: C.Y. Ito, W.L. Stanford

Other (conducted experiments and analyzed data): J.P. Howard

Disclosure of Potential Conflicts of Interest

A.J. Ruthenburg has ownership interest (including stock, patents, etc.) in Epicypher Inc. and is a consultant/advisory board member for the same. No potential conflicts of interest were disclosed by the other authors.

Deep sequencing has revealed that epigenetic modifiers are the most mutated genes in acute myeloid leukemia (AML). Thus, elucidating epigenetic dysregulation in AML is crucial to understand disease mechanisms. Here, we demonstrate that metal response element binding transcription factor 2/polycomblike 2 (MTF2/PCL2) plays a fundamental role in the polycomb repressive complex 2 (PRC2) and that its loss elicits an altered epigenetic state underlying refractory AML. Unbiased systems analyses identified the loss of MTF2–PRC2 repression of MDM2 as central to, and therefore a biomarker for, refractory AML. Thus, immature MTF2-deficient $CD34^{+}CD38^{-}$ cells overexpress MDM2, thereby inhibiting p53 that leads to chemoresistance due to defects in cell-cycle regulation and apoptosis. Targeting this dysregulated signaling pathway by MTF2 overexpression or MDM2 inhibitors sensitized refractory patient leukemic cells to induction chemotherapeutics and prevented relapse in AML patient-derived xenograft mice. Therefore, we have uncovered a direct epigenetic mechanism by which MTF2 functions as a tumor suppressor required for AML chemotherapeutic sensitivity and identified a potential therapeutic strategy to treat refractory AML.

Significance: MTF2 deficiency predicts refractory AML at diagnosis. MTF2 represses MDM2 in hematopoietic cells and its loss in AML results in chemoresistance. Inhibiting p53 degradation by overexpressing MTF2 *in vitro* or by using MDM2 inhibitors *in vivo* sensitizes MTF2-deficient refractory AML cells to a standard induction-chemotherapy regimen.

Introduction

Standard induction chemotherapy has been the first-line therapeutic to treat acute myeloid leukemia (AML) for about 40 years. Although standard induction chemotherapy can induce remission in most patients with AML, more than 30% of patients are unresponsive to treatment. Unfortunately, as many as 60% to 90% of patients with refractory AML will not survive their disease regardless of additional therapies (1). To move beyond generalized treatments, targeted therapeutics and biomarkers are actively being pursued to customize treatment regimens to attain complete remission and improve survival rates. Despite recent advances in genetic markers that stratify patients with AML into favorable, intermediate, and adverse risk categories, patients with refractory AML are found across all risk groups (2). This suggests that a nonmutational mechanism plays an important role in driving refractory AML. This hypothesis is further supported by insightful deep-sequencing studies which revealed that many of the common AML driver mutations are in epigenetic modifiers (3). Although these studies have relied heavily on DNA sequencing to identify key mutations, RNA expression levels and the epigenetic regulation within refractory AML cells have largely been overlooked.

Recent studies have shown that altered polycomb repressive complex 2 (PRC2)–mediated histone H3 lysine 27 trimethylation (H3K27me3) can predict disease outcome and survival in some cancers (4, 5). Yet, the mechanism by which H3K27me3-mediated epigenetic regulation affects cancer cell behavior, and thus patient survival, has not been well elucidated. In addition to the methyltransferase activity provided by either EZH1 or EZH2, SUZ12 and EED are core PRC2 proteins essential for function and complex stability. However, the PRC2 core proteins do not encode DNA binding activity, which is provided by accessory proteins such as polycomblike (PCL) family members (6). Thus, the prototypical

role of PRC2 accessory proteins is to recruit the PRC2 to chromatin, and their tissue-specific expression is thought to drive lineage-specific H3K27me3 methylation. MTF2/PCL2 was recently demonstrated to recruit the PRC2 to DNA regions with a high density of unmethylated CpGs resulting in chromatin conformation–dependent binding (7). In embryonic stem cells (ESC), MTF2 functions as a prototypical PRC2 accessory protein to recruit PRC2 to the extended pluripotency network gene promoters, leading to increased H3K27me3 methylation and repression of the pluripotency network to enable ESC differentiation (6). In contrast, in hematopoietic cells, MTF2 behaves more similarly to a core PRC2 component because its loss reduces SUZ12 and EZH1/2 expression and global H3K27me3 levels (8).

Although mutational and expression studies in AML are generally performed on whole bone marrow (BM) samples, we reasoned that investigating AML cell behavior would be challenging in heterogeneous bulk BM populations containing both mature and immature cells. Therefore, to examine the role of PRC2-mediated epigenetic repression in AML, we fractionated primary AML patient-derived diagnostic samples using CD34 and CD38 markers. This strategy revealed that at diagnosis, total H3K27me3 levels in $CD34^{+}CD38^{-}$ cells are markedly reduced in refractory AML patient samples due to a loss of MTF2 expression. Using an unbiased systems approach to dissect the underlying molecular networks that drive refractory AML, we discovered that the MDM2–p53 axis is regulated by MTF2 and that inhibiting MDM2 reverses MTF2–PRC2-mediated chemoresistance associated with refractory AML.

Results

Patients with MTF2 Deficiency Respond Poorly to Induction Chemotherapy

To determine whether H3K27me3 levels vary among patients with AML, we analyzed the global H3K27me3 levels of this repressive histone mark by flow cytometry within sorted $CD34^{+}CD38^{-}$, $CD34^{+}CD38^{+}$, $CD34^{+}$, and bulk cells from 32 diagnostic AML BM aspirates isolated from patients who underwent induction therapy (Fig. 1A; Supplementary Fig. S1A). Strikingly, we identified two patient groups based on total H3K27me3 levels: one with levels similar to matched normal immunophenotypic BM cells and the other with markedly reduced levels. Independent clinical patient follow-up performed in a blinded manner revealed that reduced H3K27me3 levels in diagnostic AML cells can predict nonresponders to induction therapy. However, the levels of H3K27me3 within the immature $CD34^{+}CD38^{-}$ population, which has been reported to enrich for leukemic stem cells (LSC; ref. 9), were the best indicator and predictor of therapeutic response (Supplementary Fig. S1B). In fact, analysis of the disease progression of this patient cohort found patients with H3K27me3-reduced $CD34^{+}CD38^{-}$ cells generally failed to achieve complete remission, otherwise referred to as nonresponders or patients with refractory AML (Fig. 1B and C; Supplementary Table S1). Furthermore, reduced H3K27me3 levels within patient $CD34^{+}CD38^{-}$ cells predicted poor patient survival based on our observation that the mean survival time of patients with normal levels of H3K27me3 (i.e., H3K27me3 basal) was three times longer than patients with reduced H3K27me3 levels (Fig. 1D; Supplementary Tables S2 and S3). To ensure the specificity of the H3K27me3 antibody (clone CST C36B11), we

performed internal standard calibrated chromatin immunoprecipitation (ICeChIP; ref. 10), which demonstrated the high specificity of this antibody (Supplementary Fig. S1C).

Next, we used RT-qPCR to test whether there is a correlation between H3K27me3 levels and PRC2 member expression. Linear regression analysis revealed a highly significant correlation between H3K27me3 levels and *MTF2* mRNA expression ($R^2 = 0.9416$) within the patient cohort $CD34^+CD38^-$ cells (Fig. 1E; Supplementary Fig. S2). However, the correlation between H3K27me3 levels and other PRC2 members was significant but much weaker (Fig. 1F and G; Supplementary Fig. S2). Reduced *MTF2* mRNA expression within patient $CD34^+CD38^-$ cells was also associated with poor response to standard induction chemotherapy (Fig. 1H and I) and poor survival (Supplementary Fig. S3A and S3B). Cytogenetic analysis revealed that the local patient cohort consisted of patients with AML belonging to each of the three European LeukemiaNet (ELN) risk categories (Supplementary Fig. S3C). Within the favorable cytogenetics category, *MTF2* levels further stratified patients based on overall survival (Supplementary Fig. S3D); however, this was not found to be the case in the intermediate cytogenetics category (Supplementary Fig. S3E). These results were further validated using The Cancer Genome Atlas (TCGA; ref. 11) data set in which patients with AML received an induction therapy regimen similar to the treatment given to our cohort. Kaplan–Meier analysis of the TCGA data set revealed that patients with reduced levels of *MTF2* within bulk BM cells had reduced overall survival (OS), whereas altered expression of other PRC2 members had no significant effect on patient outcome (Supplementary Fig. S3F-S3I; Supplementary Table S4). Furthermore, multivariate analysis using the TCGA data set confirmed that *MTF2* expression is a novel risk factor that can predict OS (Supplementary Table S5).

Considering *MTF2* is rarely mutated in AML, we analyzed the *MTF2* promoter for evidence of hypermethylation and discovered that at least one of the two CpG islands in the *MTF2* promoter was hypermethylated in MTF2-deficient AML (MD-AML) samples, whereas neither CpG island was methylated in healthy BM (H-BM) or AML samples with normal (basal) MTF2 levels (B-AML; Supplementary Fig. S4A). The close correlation between MTF2 expression and H3K27me3 levels led us to test whether downregulation of MTF2 is sufficient to reduce H3K27me3 levels. Thus, human umbilical cord blood–derived (UCB) $CD34^+CD38^-$ cells were transduced with two different *MTF2* shRNA GFP-encoded lentiviruses. Flow cytometry analysis of H3K27me3 levels in GFP^+cells revealed markedly reduced H3K27me3 within 96 hours of MTF2 knockdown (Fig. 1J and K). Further investigation demonstrated that MTF2 knockdown results in reduced abundance of the PRC2 core proteins EZH1, EZH2, and SUZ12 (Supplementary Fig. S4B), but their mRNA levels were not affected (Supplementary Fig. S4C), suggesting that reduced MTF2 affects PRC2 levels posttranscriptionally, resulting in decreased H3K27me3. In contrast, ectopic expression of MTF2 in MTF2-deficient $CD34^+CD38^-$ AML cells reestablished global H3K27me3 levels (Supplementary Fig. S5A-S5D), further demonstrating that MTF2 expression dictates H3K27me3 levels in hematopoietic progenitors and AML.

We next used chromatin immunoprecipitation sequencing (ChIP-seq) to investigate the changes in H3K27me3 levels triggered by MTF2 deficiency. To aid in relative H3K27me3 quantification across samples, *Drosophila* chromatin spike-in controls were added to the

samples, and H3K27me3 signal was normalized to total Histone H3 ChIP-seq signal that was performed in parallel. Although there are no differences in human total Histone H3 reads per *Drosophila* spike-in read between the various samples, human H3K27me3 reads per *Drosophila* spike-in read were reduced by 10-fold in the refractory AML patient samples compared with induction therapy–responsive MTF2 basal samples, reflecting the dramatic reduction in H3K27me3 in MTF2-deficient AML samples (Supplementary Fig. S6). A similar reduction in H3K27me3 reads per *Drosophila* spike-in read was observed in MTF2-knockdown $CD34^+CD38^-$ BM cells compared with the scramble shRNA control $CD34^+CD38^-$ BM cells. Principal component analysis and hierarchic clustering of H3K27me3 revealed that MTF2 knockdown $CD34^+CD38^-$ BM cells cluster close to refractory patient $CD34^+CD38^-$ BM cells, whereas scramble shRNA control $CD34^+CD38^-$ BM cells cluster with $CD34^+CD38^-$ BM cells from induction therapy–responsive patients (Fig. 1L and M). Taken together, these results demonstrate that MTF2 deficiency and reduced H3K27me3 levels in immature $CD34^+CD38^-$ cells correlate with refractory AML. Moreover, MTF2 deficiency within healthy $CD34^+CD38^-$ cells triggers an H3K27me3 landscape similar to that found within refractory $CD34^+CD38^-$ AML cells (Fig. 1L and M).

MTF2 Loss Drives Resistance to Standard Induction-Therapy Drugs

To test whether MTF2 deficiency confers resistance to standard induction therapy, UCB-derived Lin^-CD34^+ hematopoietic progenitors and AML patient–derived Lin^-CD34^+ leukemic cells with normal (basal) levels of MTF2 (B-AML) were transduced with *MTF2* shRNA GFP-tagged lentiviruses. GFP^+ viable cells were sorted 72 hours after transduction and then treated with the induction-therapy drugs daunorubicin or cytarabine. Forty-eight hours later, less than 6% of the scramble shRNA control UCB Lin^-CD34^+ hematopoietic progenitors survived, whereas more than 60% of MTF2 knockdown UCB Lin^-CD34^+ cells were viable (Fig. 2A and B; Supplementary Fig. S7A and S7B). Similarly, more than 25% of MTF2 knockdown B-AML cells were viable, whereas only about 1% of the scramble control B-AML cells survived (Fig. 2C and D; Supplementary Figs. S8A, S8B, and S9). Furthermore, nearly two thirds of the viable MTF2 knockdown (KD) UCB Lin^-CD34^+ cells and more than 50% of the MTF2 knockdown B-AML cells were $PCNA^+$, demonstrating that MTF2-deficient cells continue to proliferate despite chemotherapy treatment (Fig. 2E-H; Supplementary Fig. S8C and S8D; Supplementary Fig. S10). Moreover, at least 25% of cells were BrdUrd-positive in MTF2 knockdown B-AML cells following induction drug treatment, and more than 50% of these cells maintained their cycling profile based on their DNA content, compared with scramble control cells, of which only 4% incorporated BrdUrd and 17% were still cycling (Supplementary Figs. S11 and S12). Considering both daunorubicin and cytarabine target proliferating cells by inducing DNA damage (12, 13), we examined DNA damage accumulation in scramble and *MTF2* shRNA–transduced UCB Lin^-CD34^+ and B-AML Lin^-CD34^+ cells over a 48-hour period, during which the samples were treated with either induction drug. DNA damage accumulation was assessed using the alkaline comet assay, where the Olive moment (product of the tail length and the fraction of total DNA in the tail) analysis was blinded. Across all time points, the highest levels of DNA damage were found in the scramble control UCB Lin^-CD34^+hematopoietic progenitors (Fig. 2I and J; Supplementary Fig. S7C and S7D) and scramble control B-AML leukemic cells (Fig. 2K and L). Conversely, rescuing MTF2 expression in $CD34^+CD38^-$ cells from

refractory MD-AML cells by lentivirus-induced MTF2 expression sensitized refractory AML cells to daunorubicin and cytarabine, with viability dropping to negligible levels by 48 hours (Fig. 2M and N; Supplementary Figs. S13 and S14). Thus, MTF2 deficiency is sufficient to confer a refractory phenotype because inducing MTF2 loss in UCB $Lin^{-}CD34^{+}$ hematopoietic progenitors or chemoresponsive leukemic (B-AML) cells renders them chemoresistant and able to proliferate despite DNA damage, whereas MTF2 rescue in refractory AML cells leads to chemosensitivity.

Dual Inhibition of EZH1 and EZH2 Methyltransferase Activity Confers Resistance to Standard Induction-Therapy Drugs

As shown in Supplementary Fig. S4, MTF2 silencing leads to reduced PRC2 core protein abundance including the methyltransferases EZH1 and EZH2, resulting in reduced global H3K27me3. To determine whether loss of core PRC2 proteins phenocopies MTF2-mediated chemoresistance, we first knocked down the core PRC2 proteins EED or SUZ12 within UCB $Lin^{-}CD34^{+}$ cells and treated them with daunorubicin or cytarabine over 48 hours. Although less than 1% of the scramble transduced cells were viable 48 hours after treatment with daunorubicin or cytarabine, 60% or more of SUZ12 knockdown and EED knockdown $Lin^{-}CD34^{+}$ cells remained viable (Supplementary Fig. S15).

Although EZH2 is the primary PRC2 methyltransferase in adult hematopoietic cells, EZH1 compensates for EZH2 loss (14); thus, we investigated whether inhibition of the methyltransferase activity of these enzymes would confer resistance to induction-therapy drugs. Both UCB $Lin^{-}CD34^{+}$and $Lin^{-}CD34^{+}$ leukemic cells from 2 different patients with AML with normal (basal) levels of MTF2 (B-AML) and H3K27me3 were pretreated with the dual EZH1/EZH2 inhibitor UNC1999 (15) or EZH2 inhibitor EPZ005687 (16) for 3 days followed by treatment with daunorubicin or cytarabine for 48 hours. Interestingly, whereas less than 2% of the EZH2 inhibitor–treated cells were viable 48 hours after daunorubicin or cytarabine treatment, more than 65% and 25% of UCB $Lin^{-}CD34^{+}$ and B-AML cells, respectively, treated with the dual EZH1/2 inhibitor UNC1999 were viable (Fig. 2O-R; Supplementary Fig. S16). Furthermore, more than 50% of the UNC1999-treated viable cells were $PCNA^{+}$ (Fig. 2S-V) and showed the lowest amount of DNA damage accumulation across all time points (Fig. 2W-Z). Taken together, these results show that dual loss of EZH1 and EZH2, but not EZH2 alone, which had been recently suggested (5), is required to confer resistance to standard induction therapy within hematopoietic progenitors and AML cells.

MTF2 Gene Regulatory Network Regulates MDM2–p53 Expression

To identify potential molecular mechanisms underlying the poor therapeutic response in MTF2-deficient cells and altered DNA damage response (DDR), we knocked down MTF2 in UCB $Lin^{-}CD34^{+}$ cells by shRNA lentiviral transduction and performed RNA sequencing (RNA-seq). Enrichment map analysis of the transcriptomic data revealed DDR, antiapoptosis, and cell-cycle pathways were affected (Fig. 3A). Further dissection of the affected DDR transcripts showed numerous genes belonging to various DNA repair pathways were upregulated within the MTF2-deficient $Lin^{-}CD34^{+}$ hematopoietic progenitors compared with the scramble control, consistent with the reduced DNA damage

observed in the MTF2-deficient Lin$^-$CD34$^+$ hematopoietic progenitors following induction treatment (Supplementary Fig. S17A and S17B). To identify targets of the MTF2–PRC2 complex, we integrated the H3K27me3 ChIP-seq (Fig. 1L and M) with the *MTF2* knockdown RNA-seq data (Fig. 3A). The resultant MTF2–PRC2 gene regulatory network (GRN) in human Lin$^-$CD34$^+$ hematopoietic progenitors revealed the oncogenic pathways repressed by MTF2 included the PI3K and p53 pathways that regulate cell cycle, apoptosis, DDR, and chemoresistance (Fig. 3B). Although *TP53* is not a direct target of MTF2–PRC2, the gene encoding the E3-ubiquitin ligase MDM2 that targets p53 for degradation (17) is a direct target. Thus, the p53 module within the MTF2 GRN predicts that MTF2 deficiency leads to MDM2 overexpression, resulting in p53 degradation (Fig. 3C).

Indeed, ChIP-seq analysis demonstrated that MTF2 deficiency leads to loss of H3K27me3 at the *MDM2* locus, whereas total H3 levels were unaltered (Fig. 3D), with concomitant increased *MDM2*mRNA levels observed by RNA-seq (Fig. 3E). The MTF2–PRC2 GRN was validated via RT-qPCR and ChIP-qPCR (Fig. 3F and G; Supplementary Fig. S17C and S17D; Supplementary Table S6). The ChIP-qPCR validation was confirmed using both formaldehyde cross-linked ChIP (X-ChIP) and Native ChIP strategies (Supplementary Fig. S18). Functional validation using imaging flow cytometry showed that MTF2 knockdown UCB Lin$^-$CD34$^+$ cells had high MDM2 and low p53 levels (Fig. 3H; Supplementary Fig. S19A-S19C). Therefore, we hypothesized that MDM2 inhibitors would restore p53 levels in MTF2-deficient cells. Strikingly, p53 levels within MTF2 knockdown UCB Lin$^-$CD34$^+$ hematopoietic progenitors and Lin$^-$CD34$^+$ leukemic cells from refractory patient BM aspirates (MD-AML) were rescued by treatment with Nutlin3A or MI-773, which block MDM2–p53 interaction (refs. 18, 19; Fig. 3H; Supplementary Fig. S19). Furthermore, cell-cycle and PCNA analyses revealed that rescuing p53 levels using MDM2 inhibitors within MTF2-deficient UCB Lin$^-$CD34$^+$ cells decreased their proliferation rate and shifted cells into the G_0–G_1 cell-cycle stage (Supplementary Fig. S20). To test whether MTF2 regulates the MDM2–p53 axis in refractory AML patient BM cells, MTF2 expression was rescued within four MTF2-deficient Lin$^-$CD34$^+$ refractory patient BM samples (MD-AML1–4) by lentivirus-mediated MTF2 expression; this resulted in MDM2 repression and elevated p53 protein levels (Supplementary Fig. S21). Taken together, these results indicate that MTF2 regulates p53 levels via transcriptional repression of MDM2 and that MDM2 inhibitors rescue p53 levels in MTF2-deficient cells.

MDM2 Inhibitors Activate the p53 Program in MTF2-Deficient Cells Independent of HOX Gene Expression

Polycomb proteins have long been known as critical negative regulators of homeotic (HOX) gene expression (20). As indicated above, reduced EZH2 expression has recently been suggested to confer chemoresistance, mediated in part by derepression of HOXA9 and HOXB7 (5). Göllner and colleagues identified a HOXA9 gene signature using Gene Set Enrichment Analysis (GSEA) in a chemoresistant AML cell line, MV4–11R, compared with the parental cell line (5). In contrast, GSEA demonstrated a negative HOXA9 enrichment score for our MTF2 knockdown UCB Lin$^-$CD34$^+$ cell RNA-seq data (normalized enrichment score: −1.269 and −1.138, SH3 and SH7 knockdowns, respectively), suggesting that chemoresistance in MTF2-deficient cells is independent of HOX-driven mechanisms.

Considering the negative enrichment scores, we questioned whether HOXA9 and HOXB7 are derepressed in MTF2 knockdown cells; in fact, HOXA9 and HOXB7 protein levels as measured by flow cytometry were increased by 0.7-fold or less in MTF2 knockdown cells (Supplementary Fig. S22A and S22B).

To test whether MDM2 inhibition results in changes in p53 targets and *HOX* gene mRNA levels, we treated MTF2 knockdown UCB $Lin^{-}CD34^{+}$ cells and MD-AML $Lin^{-}CD34^{+}$ cells with MDM2 inhibitors for 24 hours and analyzed *HOXA9, HOXB7, PUMA*, and *CDKN1A* expression by RT-qPCR. Although no change in *HOX* gene expression was observed, a marked increase in p53 target genes *PUMA* and *CDKN1A* was detected (Supplementary Fig. S22C-S22F), consistent with the increased p53 expression upon MDM2 inhibitor treatment in MTF2-deficient cells (Fig. 3H; Supplementary Fig. S19). These data demonstrate that although MTF2 deficiency results in the loss of p53 and repression of its target genes and an increase in HOX genes, treatment with MDM2 inhibitors rescues the levels of p53 and its targets without affecting the expression of other PRC2 targets such as *HOX* genes.

Targeting the MDM2/p53 Network Module Sensitizes MTF2-Deficient Refractory AML to Standard Induction-Chemotherapy Drugs

Under normal circumstances, activation of the p53 pathway inhibits the propagation of cells that carry damaged DNA. In AML, inactivation of p53 is associated with chemoresistance, refractory disease, adverse risk group, and poor survival (11). We therefore hypothesized that rescuing p53 levels in MTF2-deficient UCB $Lin^{-}CD34^{+}$ cells with MDM2 inhibitors would sensitize them to standard induction-therapy drugs. To test this hypothesis, we transduced and sorted viable GFP^{+}MTF2 knockdown $Lin^{-}CD34^{+}$ hematopoietic cells as above and treated them with daunorubicin or cytarabine in combination with the MDM2 inhibitors Nutlin3A or MI-773 and then assayed DNA damage accumulation and cell viability. Importantly, MTF2-deficient UCB $Lin^{-}CD34^{+}$ cells exposed to the dual treatment of an MDM2 inhibitor with an induction chemotherapeutic exhibited the same amount of DNA damage accumulation as that found within scramble controls and were sensitized to induction-therapy drugs (Fig. 4A-C). Moreover, by 48 hours, refractory MD-AML cells underwent apoptosis when treated with either daunorubicin or cytarabine in combination with Nutlin3A or MI-773, comparable to induction therapy–responsive MTF2 B-AML cells (Fig. 4D and E). Interestingly, the 24-hour time point demonstrates that Nutlin3A is more efficient at sensitizing MTF2-deficient refractory AML cells to daunorubicin than MI-773, whereas the 1 μmol/L dose of MDM2 inhibitors alone had minimal effect on viability (Supplementary Fig. S23).

Combination Treatment of MDM2 Inhibitor plus Induction Drugs Improves Survival of MTF2-Deficient PDX Mice

The *in vitro* results led us to further test this combination therapy regimen (standard induction drugs plus MDM2 inhibition) *in vivo*. Mindful of the disparity between preclinical and clinical trial results (21), we designed a preclinical study that would closely mirror a clinical trial. Thus, we incorporated the following principles: AML patient-derived xenograft (PDX) mice would be treated only after the mice presented with a substantial leukemic

burden, the efficacy of combination therapy would be compared against standard induction chemotherapy, and the study would be blinded. NOD/SCID IL2Rγ^{null} (NSG) mice were conditioned by sublethal irradiation and injected with either chemoresponsive B-AML or refractory MD-AML PDX cells. Once the transplanted mice presented with ≥20% $CD45^+CD33^+$ leukemic blasts in their peripheral blood, the mice were randomized into 4 groups, which were treated with either vehicle control, Nutlin3A, induction therapy, or combination therapy (induction therapy plus Nutlin3A). Although mice belonging to the chemoresponsive B-AML PDX cohort did not respond to vehicle control or Nutlin3A alone, the B-AML PDX mice treated with induction therapy or combination therapy survived until the experiment was terminated at 16 weeks after treatment (Supplementary Fig. S24; Supplementary Table S7). However, within the cohort of mice engrafted with refractory MD-AML PDX cells, only the mice treated with combination therapy survived until the experiment was terminated at 16 weeks after treatment (Fig. 4F; Supplementary Table S7). The weights of mice belonging to the refractory AML cohort were monitored throughout the study and reflected their survival, with weights plummeting during the 5-day treatment; only combination therapy–treated mice regained their weight and recovered (Fig. 4G). Wright–Giemsa staining of BM cells harvested at endpoint from the refractory cohort showed a stark contrast between the immature blast cells isolated from induction therapy–treated mice and the differentiated BM cells isolated from the combination therapy–treated mice (Fig. 4H). Flow cytometry analysis also confirmed a dramatic loss in the blast-containing $CD45^+CD33^+$ and $CD34^+CD38^-$ populations in the combination-therapy cohort (Supplementary Fig. S25; Supplementary Table S7).

To test whether the remaining PDX cells in the combination- treated mice within the MD-AML–refractory cohort retained residual disease, we performed secondary transplants without additional treatment. The secondary transplants showed no evidence of AML during the 16-week posttransplantation observation period, after which the experiment was terminated. Flow cytometry analysis of BM cells from secondary transplants revealed that the transplanted cells were capable of multilineage engraftment, suggesting that the combination therapy targeted bulk AML cells and LSCs while sparing some normal Lin^-CD34^+ stem and progenitor cells (Supplementary Fig. S26; Supplementary Table S8). Finally, flow-cytometric analysis showed the combination therapy–treated mice and their secondary transplant recipients had reduced BM cellularity, compared with DMSO, Nutlin3A alone, or induction-treated mice cohorts (Fig. 4I).

Discussion

Altered epigenetic states such as H3K27me3 deficiency are observed in different types of cancers and have been correlated with poor outcome (4, 22). However, the mechanism underlying H3K27me3 deficiency and how it contributes to a poor prognosis has been unclear. Here we establish, using UCB Lin^-CD34^+ and patient-derived Lin^-CD34^+ leukemic cells, that MTF2/PRC2 epigenetically regulates the MDM2–p53 axis. Thus, MTF2 loss results in MDM2 upregulation and decreased p53-mediated apoptosis that contributes to refractory AML, which is overcome by treating the cells with induction drugs plus an MDM2 inhibitor. Furthermore, we demonstrate that MTF2 stabilizes PRC2. Therefore, loss

of MTF2, EED, or SUZ12 results in chemoresistance, whereas loss of the methyltransferase EZH2 alone is insufficient to confer chemoresistance.

A recent study by Göllner and colleagues also found that low levels of H3K27me3 correlate with poor OS in AML (5); however, there are marked differences in the mechanistic explanations for this observation between the two studies. In short, Göllner and colleagues find the loss of EZH2 leads to derepression of HOXA9 and HOXB7, which then drives chemoresistance (5). Interestingly, there are many technical differences between the two studies that likely lead to the different conclusions reached. The primary difference is that although we utilized primary UCB cells and PDX-expanded patient-derived diagnostic samples without regard to specific leukemogenic driver mutations, Göllner and colleagues performed their mechanistic experiments using AML cell lines. In particular, they analyzed a drug-resistant FLT3-ITD$^+$ AML cell line, MV4–11R, which demonstrated reduced EZH2 and H3K27me3 compared with the MV4–11 parental line (5). Interestingly, MV4–11R cells also encode *TP53* mutations known to affect drug sensitivity. Thus, MV4–11R cells have undergone selective pressures leading to MDM2–p53 independent drug resistance, in which *HOXA9* and *HOXB7* play a role. Consistent with this point, we do not observe the HOXA9 gene signature in MTF2-deficient cells that was identified in MV4–11R cells. Göllner and colleagues also reported EZH2 inhibition alone drives chemoresistance (5). In contrast, we find that the refractory phenotype is only manifested when the methyltransferase activities of both EZH1 and EZH2 are inhibited. This is consistent with the fact that EZH1 can compensate for EZH2 within adult BM (14) and our finding that MTF2 is required for EZH1 and EZH2 expression in Lin$^-$CD34$^+$ cells. It should be noted that the inhibitor DZNep is known to have poor specificity to EZH2 (23), likely explaining Göllner and colleagues' conclusion that EZH2 inhibition alone drives chemoresistance (5). Moreover, we demonstrate that sensitizing chemoresistant AML cells to induction drugs via MDM2 inhibitors is independent of alterations in *HOXA9* and *HOXB7* expression, the mechanism implicated in EZH2-mediated chemoresistance by the authors (5). Finally, while using flow-cytometric analysis of CD34$^+$38$^-$ cells from diagnostic patient samples, we found closer to 50% of diagnostic samples have low H3K27me3; Göllner and colleagues found more than 75% of patient samples have low H3K27me3 using IHC of bulk BM samples, suggesting the biomarker detection method is important to identify chemoresistant patients (5).

Seminal studies in AML defined LSCs or leukemia initiating cells (LIC) based on their ability to transplant the disease in sublethally irradiated mice. Using the limiting dilution assay, it has been shown that although LSCs/LICs are highly enriched within CD34$^+$CD38$^-$ cells, LSCs/LICs are also prevalent in other immunophenotypic AML subpopulations, albeit at significantly lower frequencies (24). We therefore profiled the H3K27me3 levels within the different immunophenotypic AML subpopulations from 32 diagnostic AML samples and observed that H3K27me3 levels can vary among the different BM subpopulations (Supplementary Fig. S1A and S1B). H3K27me3 levels within the CD34$^+$CD38$^-$ population best predicted response to induction therapy. For the first time, we demonstrate that reduced expression of the PRC2 protein MTF2 and low H3K27me3 levels within CD34$^+$CD38$^-$ AML cells prospectively identify refractory AML at diagnosis and provide a direct mechanism for MTF2- and PRC2-mediated chemoresistance.

AML is a clinically heterogeneous disease, with marked differences in survival following chemotherapy, based on blast cell morphology, age, and cytogenetics. Although therapeutic advances have lagged for nearly four decades, an increased number of prognostic factors have been identified that can predict patient OS, and these biomarker discoveries have driven the field's understanding of AML biology and the development of new therapeutic targets. In our study, using both our local patient cohort and the reported TCGA survival data, we demonstrate that MTF2 deficiency correlated with poor OS (Supplementary Fig. S3). Multivariate analysis of the TCGA data revealed low *MTF2* expression as a prognostic marker when adjusted for effects of age, white blood cells (WBC), and cytogenetics. This is the case for *TP53* wild-type patients ($n = 153$) and when the analysis is extended to all patients ($n = 165$; Supplementary Tables S5 and S9). Furthermore, MTF2 expression is capable of further stratifying patients with favorable cytogenetics (Supplementary Fig. S3). In contrast, at least in bulk BM samples, *MDM2* transcript levels are not predictive of OS (Supplementary Tables S10 and S11). This may be explained by the fact that in bulk BM there is a weak inverse correlation between *MDM2* and *MTF2* transcript levels (Pearson $r = -0.216$, $P = 0.005$; Spearman $s = -0.243$, $P = 0.002$), suggesting a nonlinear inverse correlation. However, in $CD34^+CD38^-$ cells, we observe a stronger inverse correlation between MTF2 and MDM2 protein levels (Supplementary Figs. S19 and S21).

Mechanistically, we demonstrated that *MTF2* repression is due to hypermethylation of its promoter, thus leading to derepression of *MDM2*, p53 degradation, and ensuing aberrant apoptosis, cell cycling, and DDR. Furthermore, rescuing MTF2 expression in primary MTF2-low LSC-enriched populations reversed chemoresistance, whereas knockdown of MTF2 in UCB Lin^-CD34^+hematopoietic cells and AML Lin^-CD34^+ leukemic cells with normal levels of MTF2 induced resistance to induction-chemotherapy drugs. Because MTF2 plays a fundamental role in chemoresistance, MTF2 deficiency is not only correlative, but predictive of refractory AML. We also illustrate that the refractoriness observed within patients with AML with low H3K27me3 levels is driven by high MDM2 and low p53 levels.

Recent deep-sequencing studies have suggested that epigenetic alterations and changes in the epigenome, which are commonly observed across all cancers, are often associated with genetic mutations or transcriptional alterations of many genes related to cancer progression (25). Hence, targeting the epigenome is currently an area of intense research to improve upon standard-of-care chemotherapies (26, 27). Here, we demonstrate the reversibility of the AML epigenetic state by genetic manipulation of MTF2 and the use of small-molecule inhibitors against the catalytic activity of EZH1/EZH2. Furthermore, we target the dysregulated epigenetic pathway associated with refractory AML and demonstrate that MDM2 inhibitors in combination with standard induction chemotherapy provide a promising strategy to treat chemoresistant AML, a strategy recently proposed by Carvajal and colleagues (28). Moreover, in secondary transplants using the whole marrow isolated from our combination therapy–treated mice, we observed multilineage human hematopoietic cell engraftment, but no signs of disease (Supplementary Fig. S26; Supplementary Table S7). These results suggest that combination therapy preferentially targets refractory LSCs compared with healthy hematopoietic stem and progenitor cells, although additional experiments are required to directly test this hypothesis. We posit that similar strategies may be used to target the epigenetic states of other cancers.

Although *TP53* dysfunction and mutations are typically associated with aggressive refractory disease (29, 30), large-scale deep-sequencing data sets show that only 2% to 8% of patients with AML have p53 mutations (11, 31). Therefore, our proposed combination therapy could effectively treat the majority of patients with refractory AML. However, our data predict that in the absence of MDM2 inhibitors, MTF2-deficient AML cells will cycle through induction therapy and accumulate additional mutations, potentially including *TP53* therapy-induced mutations, which could render the cells resistant to MDM2 inhibitors (32). Because MDM2 inhibitors are now in clinical trials for a number of indications including treatment of AML, it would be prudent to screen patients with AML at diagnosis for MTF2 and H3K27me3 levels in $CD34^{+}CD38^{-}$ cells by flow cytometry to prospectively identify chemoresistant AML prior to treatment to identify candidates who will benefit the most from this targeted combination therapy.

In addition to the MDM2–p53 axis, which we found to be an underlying molecular mechanism for poor therapeutic response in MTF2-deficient cells, our MTF2 GRN identified other targets and mechanisms that may contribute to chemoresistance. Given their known roles in regulating cell-cycle progression, other potential interesting therapeutic targets include p14/ARF and Rb, as they play similar roles to that of p53. The manipulation of their expression or activity could also provide new strategies to target MTF2-deficient chemoresistant cells.

Methods

Additional details are provided in the Supplementary Methods and Data files.

Animal Experiments Approval

All animal experiments were conducted with approval from the University of Ottawa Animal Care Committee, in accordance with the Canadian Council on Animal Care Standards and the Province of Ontario's Animals for Research Act. NSG mice were purchased from Jackson Labs. Mice were maintained in sterile housing conditions and given autoclaved chow and water *ad libitum*.

Patient Samples and Study Approval

All patient samples and human UCB samples used in this study were performed after written informed consent was obtained from patients. Human UCB samples were obtained from the Canadian Blood Services (Ottawa, Canada) and the Mount Sinai Hospital Research Centre for Women's and Infants' Health BioBank (Toronto, Canada). Informed consent and collection and research use of the human UCB samples were approved by the respective Research Ethics Boards and the Ottawa Hospital Research Ethics Board which operate according to the Declaration of Helsinki and the International Ethical Guidelines for Biomedical Research Involving Human Subjects. AML patient BM samples were collected after written informed consent was obtained from patients at The Ottawa Hospital. Procurement and use of AML BM patient samples for research was approved by The Ottawa Hospital Research Ethics Board, which operates according to the Declaration of Helsinki

and the International Ethical Guidelines for Biomedical Research Involving Human Subjects.

Patient Treatment and Response Analysis

Diagnostic BM samples from patients with AML were obtained after informed consent. Patients were treated as per the protocols at The Ottawa Hospital, Ontario, Canada. In addition to the usual supportive care, they received induction chemotherapy with idarubicin (12 mg/m^2 daily for 3 days) and cytarabine (200 mg/m^2/day by continuous infusion for 7 days). A BM sampling was repeated upon recovery of blood counts and/or between days 25 and 40. Responsive disease was defined as <5% BM blasts. Patients who had ≥5% BM blasts were designated as failing or resistant to induction, for the purposes of this study. These patients were then treated with a salvage chemotherapy and considered for an allogeneic hematopoietic stem cell (HSC) transplant. Patients who did achieve a complete remission proceeded to receive consolidation and were considered for an allogeneic HSC transplant.

Lentivirus Production and Transduction of Primary Cells

293T cells were seeded in 15-cm dishes (Corning Falcon). After 48 hours, cells were cotransfected with second-generation packaging lentiviral plasmids pMD2G, pPAX2, and either pGIPZ encoding shRNAs (Thermo Scientific) or pLenti overexpression vector (abm, Canada) in the presence of polyethylenimine (4.1 μmol/L) and NaCl (2.25×10^{-4} mol/L). Virus was produced using 40 to 80 15-cm dishes for each virus construct. Supernatant containing the virus was collected 48 and 72 hours after transfection and concentrated by ultracentrifugation and resuspended in a final volume of 300 μL of serum-free media. The viral titer for the pGIPZ and pLenti backbone viruses on each day of virus collection was ~10^6 and ~10^5 viral particles/μL, respectively.

UCB Lin$^-$ or Lin$^-$CD34$^+$ cells or PDX-expanded primary AML BM Lin$^-$CD34$^+$ cells were cultured in 96-well plates (Falcon) under conditions described by Csaszar and colleagues, in Iscove's modified Dulbecco's medium (IMDM) containing BIT9500, 1% penicillin and streptomycin, stem cell factor (SCF; 100 ng/mL), thrombopoietin (50 ng/mL), FLT3 (100 ng/mL), 1% glutamax, and low-density lipoprotein (1 μg/mL); and Pabst and colleagues, in IMDM containing SCF (100 ng/mL), FLT3 (50 ng/mL), IL3 (20 ng/mL), G-CSF (20 ng/mL), 10^{-4} mol/L β-mercaptoethanol, and 15% BIT, respectively (33, 34). On day 1 of infection, 200,000 cells were incubated with polybrene (Sigma; 6 mg/mL) for 2 hours at 37°C, 5% CO_2, then combined with concentrated virus at a multiplicity of infection (MOI) of 100 or 30 for pGIPZ or pLenti backbone viruses, respectively. The functional MOI was previously calculated using UCB Lin$^-$CD34$^+$ cells. Cells were centrifuged at 400 × *g* for 20 minutes, then maintained at 37°C. On day 2, the infection was repeated. The functional MOI was determined based on GFP expression measured using BDFortessa or BDAstrios on both days of virus collection. Cells were grown for 3 days using a fed-batch culture system (34) and then sorted for high GFP expression and viability by negative selection of propidium iodide (BD Biosciences) using the Beckman Coulter Astrios sorter or MoFlo sorter (Beckman Coulter). The transduction of the AML cells was always performed using fresh virus. Using this protocol, we consistently transduced more than 50% of the cells.

RNA-seq and ChIP-seq

UCB-derived $Lin^{-}CD34^{+}$ cells were transduced with either the GFP-tagged MTF2 shRNAs or a scrambled shRNA control. Transduced GFP^{+} cells were sorted 72 hours after transduction using a MoFlo sorter (Beckman Coulter). RNA was extracted from 150,000 cells per condition for RNA-seq analysis. RNA was isolated (Arcturus PicoPure Kit, LifeTech), DNase treated (Qiagen), and 2 μL of ERCC Spike-In mix (Thermo Fisher Scientific) was added to each of the GFP-tagged MTF2 shRNAs or a scrambled shRNA control. Quality of RNA was determined using a Bioanalyzer. Library preparation was performed using TruSeq Library Prep Kit (Illumina) and sequenced on a HiSeq 2000 (Illumina). Raw RNA-seq data are available in Gene Expression Omnibus (GEO; GSE98343).

For ChIP-seq, PDX-expanded $CD34^{+}CD38^{-}$ sorted cells (no lineage depletion was performed) were cross-linked with 1% formaldehyde for 10 minutes at room temperature. Samples were sheared using a Covaris sonicator (cycles/burst = 200; time: 480 minutes; temperature: 6°C to 8°C; water level: 12; peak power: 175) until DNA reached a final size of 100 to 300 bp. To ensure protein stability, the percentage of SDS in the lysis buffer was reduced to 0.1%. Upon sonication, one volume of dilution buffer (1% Triton X-100, 1.2 mmol/L EDTA, and 16.7 mmol/L Tris–HCL pH8.1) was added to neutralize the SDS. 750 ng of *Drosophila* chromatin spike-in (Active Motif) was added to each sonicated sample. Four micrograms of anti-H3K27me3 antibody (Cell Signaling Technology, c36B11) or H3 (Abcam, ab1791) was bound to preblocked protein A magnetic beads (Millipore) in combination with 2 μg of spike-in antibody (Active Motif) for 12 hours. The beads were then combined with sonicated sample containing *Drosophila* chromatin spike-in and incubated overnight. After incubation, beads were collected and washed with low-salt buffer (0.1% SDS, 1% Triton X-100, 2 mmol/L EDTA, 20 mmol/L Tris–HCL ph8.1, 150 nmol/L NaCL) and TE buffer (1 mol/L Tris–HCL ph8.0, 0.5 mol/L EDTA, 10% SDS and ddH_2O). The DNA–antibody complexes were eluted at 65°C while shaking at 1,250 g. Cross-links were reversed overnight at 65°C. Samples were treated with Proteinase K (Fisher Scientific) and RNase A (Fisher Scientific), and DNA was purified using phenol-chloroform. The purified DNA for each sample was resuspended in 15 μL. All ChIP-seq experiments were cell number normalized, and 150,000 cells per biological sample were used for each H3 and H3K27me3 ChIP experiment. Raw ChIP-seq data are available in GEO (GSE98378). Sequencing data can be found in GEO (GSE98380).

AML PDX Mouse Model and *In Vivo* Treatment

Briefly, female NSG mice (>7 week old) were sublethally irradiated with 300 Rads (Gammacell 3000) and transplanted via tail vein with 1 million bulk AML patient BM cells, which had been previously expanded and harvested from NSG mice. Upon the presence of >20% $CD45^{+}CD33^{+}$cells in the peripheral blood (~50–57 days after transplantation), mice were randomized into 4 treatment groups [$n = 6$ PDX samples (4 from refractory AML and 2 from basal AML); $n = 2$ mice per group; $n = 8$ mice total per group] and treated with (i) DMSO, (ii) Nutlin3A, (iii) induction therapy, or (iv) combination therapy. The person who administered the treatment intravenously via tail vein was blinded to the contents of the syringes. Mice belonging to the induction-therapy cohort were treated based on the

previously published 5 + 3 treatment regimen (35) with the following modifications: (i) daunorubicin was used, (ii) drugs were administered intravenously via the tail vein and delivered in 2 × 200 μL doses 30 minutes apart, (iii) mice were fed a water-rich diet consisting of ice cubes, liquid gelatin, and autoclaved chow soaked in sterile water, and (iv) bedding was changed daily to minimize exposure to excreted drugs.

Statistical Analysis

All data were expressed as mean ± SEM or SD. Data were analyzed using Prism 6.0 (GraphPad Software). Two-way ANOVA measured statistical significance between the conditions. Kaplan–Meier curves were calculated using GraphPad Prism 6.0, and significance was determined by log-rank test (Mantel–Cox). Pearson correlation was performed using SPSS v20.0. Multivariate Cox proportional hazards models were used to test the association of MDM2 and MTF2 with OS in parallel models. Age, risk cytogenetics, and WBC were included as identified important covariates in these models. The interaction between time and each of the covariates was included in the model one at a time, to assess if the effect of the given covariate is constant over time. There was no evidence for violation of proportional hazard assumption ($P > 0.1$). Adjusted hazard ratios with respective 95% confidence intervals were reported as results. SAS 9.3 was used to run the multivariable models. A P value of <0.05 was used as a cutoff to indicate statistical significance.

Supplementary Material

Refer to Web version on PubMed Central for supplementary material.

Acknowledgments

We thank the OHRI Stem Core Facility for their assistance with FACS and sequencing and the University of Ottawa/Ottawa Heart Institute Animal Care Facility for their invaluable assistance with the mouse experiments. This work was supported by operating grants from the Canadian Cancer Society Research Institute (2011-700822; 704783), Canadian Institutes of Health Research (MOP 142474), and the Cancer Research Society (CRS18330) to W.L. Stanford and C.Y. Ito, and the National Institutes of Health (R01-GM115945) to A.J. Ruthenburg. W.L. Stanford was supported by a Tier 1 Canada Research Chair in Integrative Stem Cell Biology.

References

1. Thol F, Schlenk RF, Heuser M, Ganser A. How I treat refractory and early relapsed acute myeloid leukemia. Blood 2015; 126:319–27. [PubMed: 25852056]
2. Döhner H, Estey E, Grimwade D, Amadori S, Appelbaum FR, Büchner T, et al. Diagnosis and management of AML in adults: 2017 ELN recommendations from an international expert panel. Blood 2017; 129:424–47. [PubMed: 27895058]
3. Glass J, Hassane DC, Wouters B, Kunimoto H, Avellino R, Garrett-Bakelman FE, et al. Epigenetic identity in AML depends on disruption of non-promoter regulatory elements and is affected by antagonistic effects of mutations in epigenetic modifiers. Cancer Discov 2017; 7: 868–83. [PubMed: 28408400]
4. Cai MY, Hou JH, Rao HL, Luo RZ, Li M, Pei XQ, et al. High expression of H3K27me3 in human hepatocellular carcinomas correlates closely with vascular invasion and predicts worse prognosis in patients. Mol Med 2011; 17:12–20. [PubMed: 20844838]
5. Gollner S, Oellerich T, Agrawal-Singh S, Schenk T, Klein HU, Rohde C, et al. Loss of the histone methyltransferase EZH2 induces resistance to multiple drugs in acute myeloid leukemia. Nat Med 2017; 23:69–78. [PubMed: 27941792]

6. Walker E, Chang WY, Hunkapiller J, Cagney G, Garcha K, Torchia J, et al. Polycomb-like 2 associates with PRC2 and regulates transcriptional networks during mouse embryonic stem cell self-renewal and differentiation. Cell Stem Cell 2010; 6:153–66. [PubMed: 20144788]
7. Perino M, van Mierlo G, Karemaker ID, van Genesen S, Vermeulen M, Marks H, et al. MTF2 recruits Polycomb Repressive Complex 2 by helical-shape-selective DNA binding. Nat Genet 2018; 50:1002–10. [PubMed: 29808031]
8. Rothberg JLM, Maganti HB, Jrade H, Porter CJ, Palidwor GA, Cafariello C, et al. Mtf2-PRC2 control of canonical Wnt signaling is required for definitive erythropoiesis. Cell Discov 2018; 4:21. [PubMed: 29736258]
9. Ding L, Ley TJ, Larson DE, Miller CA, Koboldt DC, Welch JS, et al. Clonal evolution in relapsed acute myeloid leukaemia revealed by whole-genome sequencing. Nature 2012; 481:506–10. [PubMed: 22237025]
10. Grzybowski AT, Chen Z, Ruthenburg AJ. Calibrating ChIP-Seq with nucleosomal internal standards to measure histone modification density genome wide. Mol Cell 2015; 58:886–99. [PubMed: 26004229]
11. Cancer Genome Atlas Research Network, Ley TJ, Miller C, Ding L, Raphael BJ, Mungall AJ, et al. Genomic and epigenomic landscapes of adult de novo acute myeloid leukemia. N Engl J Med 2013; 368:2059–74. [PubMed: 23634996]
12. Xie C, Edwards H, Xu X, Zhou H, Buck SA, Stout ML, et al. Mecha- nisms of synergistic antileukemic interactions between valproic acid and cytarabine in pediatric acute myeloid leukemia. Clin Cancer Res 2010; 16:5499–510. [PubMed: 20889917]
13. Come MG, Skladanowski A, Larsen AK, Laurent G. Dual mechanism of daunorubicin-induced cell death in both sensitive and MDR- resistant HL-60 cells. Br J Cancer 1999; 79:1090–7. [PubMed: 10098741]
14. Xie H, Xu J, Hsu JH, Nguyen M, Fujiwara Y, Peng C, et al. Poly- comb repressive complex 2 regulates normal hematopoietic stem cell function in a developmental-stage-specific manner. Cell Stem Cell 2014; 14:68–80. [PubMed: 24239285]
15. Xu B, On DM, Ma A, Parton T, Konze KD, Pattenden SG, et al. Selec- tive inhibition of EZH2 and EZH1 enzymatic activity by a small mol- ecule suppresses *MLL*-rearranged leukemia. Blood 2015 ;125:346–57. [PubMed: 25395428]
16. Knutson SK, Wigle TJ, Warholic NM, Sneeringer CJ, Allain CJ, Klaus CR, et al. A selective inhibitor of EZH2 blocks H3K27 methylation and kills mutant lymphoma cells. Nat Chem Biol 2012; 8:890–6. [PubMed: 23023262]
17. Marine JC, Lozano G. Mdm2-mediated ubiquitylation: p53 and beyond. Cell Death Differ 2010; 17:93–102. [PubMed: 19498444]
18. McCormack E, Haaland I, Venas G, Forthun RB, Huseby S, Gausdal G, et al. Synergistic induction of p53 mediated apoptosis by valproic acid and nutlin-3 in acute myeloid leukemia. Leukemia 2012; 26:910–7. [PubMed: 22064349]
19. Wang S, Sun W, Zhao Y, McEachern D, Meaux I, Barriere C, et al. SAR405838: an optimized inhibitor of MDM2-p53 interaction that induces complete and durable tumor regression. Cancer Res 2014; 74:5855–65. [PubMed: 25145672]
20. Struhl G Role of the esc+ gene product in ensuring the selective expression of segment-specific homeotic genes in Drosophila. J Embryol Exp Morphol 1983; 76:297. [PubMed: 6631324]
21. Zuber J, Radtke I, Pardee TS, Zhao Z, Rappaport AR, Luo W, et al. Mouse models of human AML accurately predict chemotherapy response. Genes Dev 2009; 23:877–89. [PubMed: 19339691]
22. Torchia J, Golbourn B, Feng S, Ho KC, Sin-Chan P, Vasiljevic A, et al. Integrated (epi)-Genomic Analyses Identify Subgroup-Specific Therapeutic Targets in CNS Rhabdoid Tumors. Cancer Cell 2016;30: 891–908. [PubMed: 27960086]
23. Fujiwara T, Saitoh H, Inoue A, Kobayashi M, Okitsu Y, Katsuoka Y, et al. 3-Deazaneplanocin A (DZNep), an inhibitor of S-adenosylmethionine-dependent methyltransferase, promotes erythroid differentiation. J Biol Chem 2014; 289:8121–34. [PubMed: 24492606]
24. Goardon N, Marchi E, Atzberger A, Quek L, Schuh A, Soneji S, et al. Coexistence of LMPP-like and GMP-like leukemia stem cells in acute myeloid leukemia. Cancer Cell 2011; 19:138–52. [PubMed: 21251617]

25. Li S, Garrett-Bakelman FE, Chung SS, Sanders MA, Hricik T, Rapa-port F, et al. Distinct evolution and dynamics of epigenetic and genetic heterogeneity in acute myeloid leukemia. Nat Med 2016; 22:792–9. [PubMed: 27322744]
26. Shih AH, Meydan C, Shank K, Garrett-Bakelman FE, Ward PS, Intlekofer AM, et al. Combination targeted therapy to disrupt aberrant oncogenic signaling and reverse epigenetic dysfunction in IDH2- and TET2-mutant acute myeloid leukemia. Cancer Discov 2017;7: 494–505. [PubMed: 28193779]
27. Kuhn MW, Song E, Feng Z, Sinha A, Chen CW, Deshpande AJ, et al. Targeting chromatin regulators inhibits leukemogenic gene expres- sion in NPM1 mutant leukemia. Cancer Discov 2016;6:1166–81. [PubMed: 27535106]
28. Carvajal LA, Neriah DB, Senecal A, Benard L, Thiruthuvanathan V, Yatsenko T, et al. Dual inhibition of MDMX and MDM2 as a therapeutic strategy in leukemia. Sci Transl Med 2018; 10: eaao3003. [PubMed: 29643228]
29. Kruiswijk F, Labuschagne CF, Vousden KH. p53 in survival, death and metabolic health: a lifeguard with a licence to kill. Nat Rev Mol Cell Biol 2015; 16:393–405. [PubMed: 26122615]
30. Prokocimer M, Molchadsky A, Rotter V. Dysfunctional diversity of p53 proteins in adult acute myeloid leukemia: projections on diagnostic workup and therapy. Blood 2017; 130:699–712. [PubMed: 28607134]
31. Patel JP, Gönen M, Figueroa ME, Fernandez H, Sun Z, Racevskis J, et al. Prognostic relevance of integrated genetic profiling in acute myeloid leukemia. N Engl J Med 2012; 366:1079–89. [PubMed: 22417203]
32. Long J, Parkin B, Ouillette P, Bixby D, Shedden K, Erba H, et al. Multiple distinct molecular mechanisms influence sensitivity and resistance to MDM2 inhibitors in adult acute myelogenous leukemia. Blood 2010; 116:71–80. [PubMed: 20404136]
33. Pabst C, Krosl J, Fares I, Boucher G, Ruel R, Marinier A, et al. Identi- fication of small molecules that support human leukemia stem cell activity ex vivo. Nat Methods 2014; 11:436–42. [PubMed: 24562423]
34. Csaszar E, Kirouac DC, Yu M, Wang W, Qiao W, Cooke MP, et al. Rapid expansion of human hematopoietic stem cells by automated control of inhibitory feedback signaling. Cell Stem Cell 2012; 10:218–29. [PubMed: 22305571]
35. Wunderlich M, Mizukawa B, Chou F-S, Sexton C, Shrestha M, Saunthararajah Y, et al. AML cells are differentially sensitive to chemotherapy treatment in a human xenograft model. Blood 2013; 121:e90–7. [PubMed: 23349390]

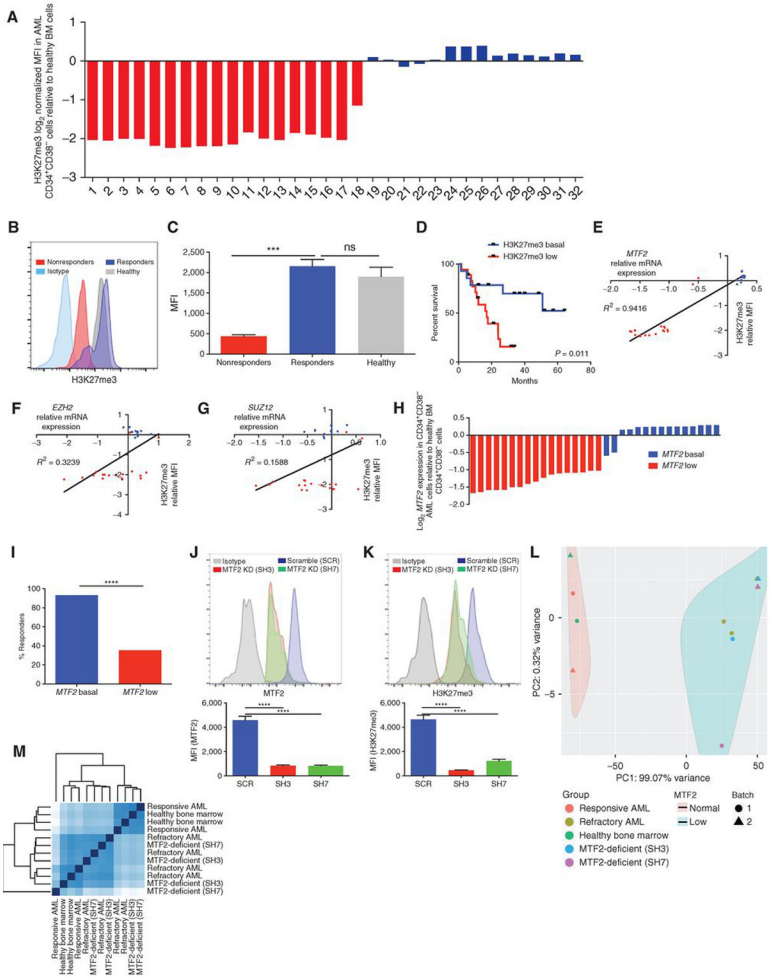

Figure 1.

MTF2 deficiency correlates with poor response to standard treatment of care. **A,** 18 of 32 diagnostic AML BM aspirates demonstrated low mean fluorescence intensity (MFI) for H3K27me3 levels by flow-cytometric analysis compared with 7 normal BM aspirates (set to 0 in the $\log_2$ scale). **B,** Representative flow cytometry histogram comparing H3K27me3 levels within the $CD34^+CD38^-$ population isolated from AML patient and healthy donor BM samples. **C,** The H3K27me3 MFI obtained from flow cytometry analysis of 32 diagnostic and 7 healthy donor BM samples demonstrates that reduced levels of H3K27me3 in $CD34^+CD38^-$ cells correlate with poor response to induction therapy. **D,** Survival analysis of the 32 patients with AML treated by induction therapy shows H3K27me3 levels within patient $CD34^+CD38^-$cells correlated with patient outcome; *P* value was calculated using log-rank (Mantel–Cox) test. **E–G,** Linear regression analysis of PRC2 complex members (**E**) *MTF2*, (**F**) *EZH2*, and (**G**) *SUZ12* revealed that only *MTF2* mRNA expression correlates strongly with H3K27me3 levels within patient cohort. **H,** *MTF2* expression within $CD34^+CD38^-$ cells isolated from the same 32 diagnostic AML BM aspirates compared with $CD34^+CD38^-$ cells from 7 healthy BM aspirates assessed by RT-qPCR. Seventeen aspirates were determined to have low levels of *MTF2* expression (<−1), and 15 aspirates were determined to have basal levels of *MTF2* expression (−1 to +1, with 0 representing the mean

of 7 healthy BMs). **I,** A double-blinded drug-response analysis determined that patients within the patient cohort with low *MTF2* expression responded poorly to standard induction chemotherapy. **J** and **K,** Knockdown (KD) of (**J**) MTF2 within umbilical cord blood $CD34^+CD38^-$ cells decreases (**K**) H3K27me3 levels, assessed by flow cytometry. **L,** Principal component analysis of spike-in normalized H3K27me3 ChIP-seq data from $CD34^+CD38^-$ cells isolated from patients with refractory AML ($n = 4$ samples), responsive patients with AML ($n = 2$ samples) or healthy BM transduced with MTF2 ($n = 4$ samples) or scramble ($n = 2$ samples) lentivirus shRNA. The H3K27me3 ChIP sequencing was performed in 2 independent batches (batch 1 = •, batch 2 = ▲). **M,** Hierarchical clustering analysis demonstrated that the MTF2-deficient $CD34^+CD38^-$ BM population clusters closely to the $CD34^+CD38^-$ population isolated from refractory AML BM aspirates. All data represent mean ± standard deviation; *, $P < 0.05$; **, $P < 0.005$; ***, $P < 0005$; ****, $P < 0.00005$ by Student *t* test.

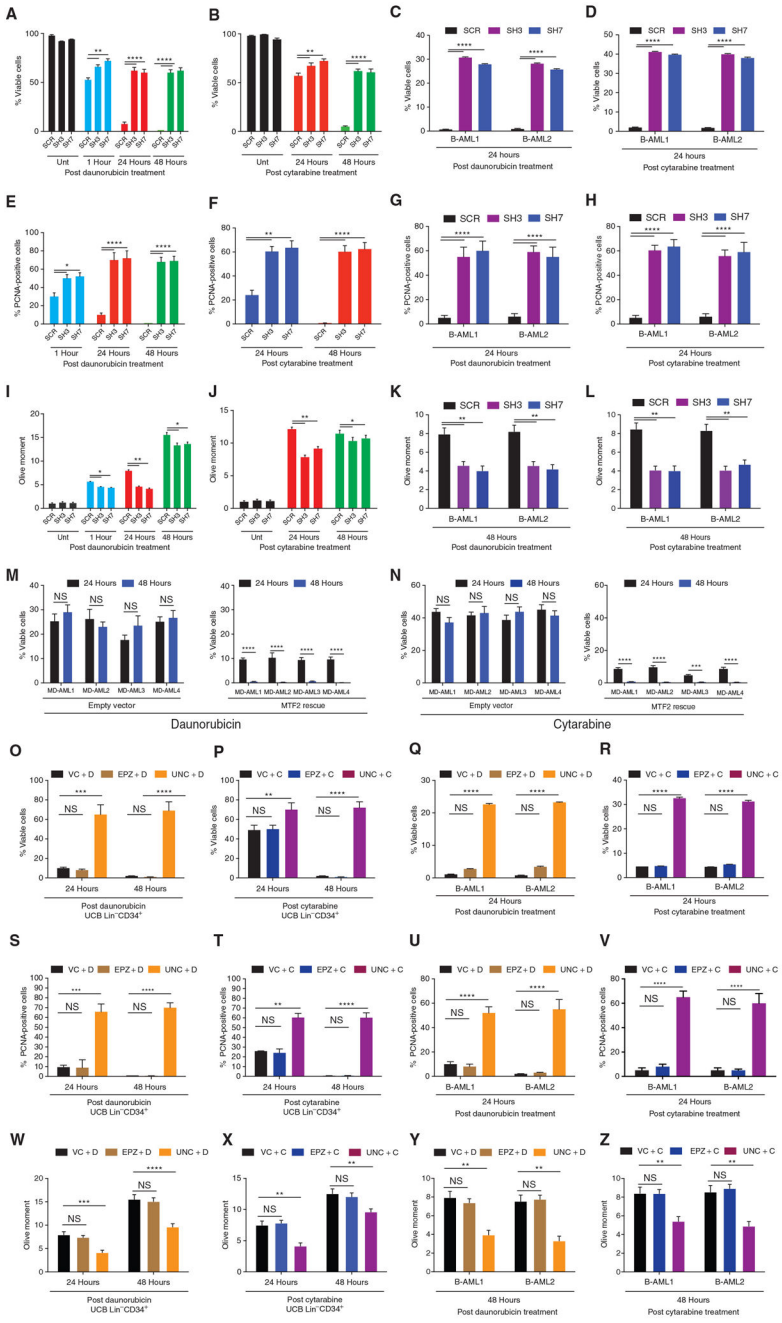

Figure 2.

MTF2 knockdown in hematopoietic progenitors or chemoresponsive leukemic cells, but not EZH2 inhibition alone, confers resistance to standard treatment of care. **A** and **B,** Viability of scramble control (SCR) and MTF2 shRNA (SH3 or SH7) KD UCB Lin^{-} CD34^{+} cells were assessed over a 48-hour time period after treatment with (**A**) daunorubicin or (**B**) cytarabine. **C** and **D,** Viability of scramble control (SCR) and MTF2 (SH3 or SH7) shRNA KD Lin^{-}CD34^{+}chemoresponsive leukemic cells isolated from MTF2-basal AML samples (B-AML) were assessed posttreatment with (**C**) daunorubicin or (**D**) cytarabine. By 24 hours after treatment, more than 25%, but less than 2%, of KD B-AML and scramble control cells,

respectively, remain viable. **E** and **F,** PCNA proliferation marker analysis of scramble control (SCR) and MTF2 shRNA (SH3, SH7) KD UCB $Lin^{-}CD34^{+}$ 48 hours after (**E**) daunorubicin or (**F**) cytarabine treatment. Viable cells from **A** and **B** were stained for PCNA, to assess cell proliferation. **G** and **H,** Proliferation analysis of scramble control (SCR) and MTF2 shRNA (SH3, SH7) KD B-AML cells 24 hours (**G**) after daunorubicin or (**H**) after cytarabine treatment. Viable cells from **C** and **D** were stained for PCNA, to assess cell proliferation. Both MTF2-deficient hematopoietic progenitors and B-AML cells continue to proliferate significantly more than control cells posttreatment. **I** and **J,** Overall DNA damage accumulation after induction treatment with (**I**) daunorubicin or (**J**) cytarabine was assessed over 48 hours via the alkaline comet assay. Blinded, ImageJ OpenComet analysis of the Olive moment was used to quantify DNA damage at the single-cell level, and although both the scramble (SCR) and MTF2 (SH3 or SH7) KD hematopoietic progenitors accumulated DNA damage over time, the MTF2 KD UCB $Lin^{-}CD34^{+}$ cells accumulated significantly less damage at each individual time point. **K** and **L,** Overall DNA damage accumulation in transduced B-AML cells after induction treatment with (**K**) daunorubicin or (**L**) cytarabine was assessed over 48 hours via the alkaline comet assay. MTF2 KD leukemic B-AML cells accumulated significantly less DNA damage than scramble controls. **M** (left), The $CD34^{+}CD38^{-}$ BM subpopulation from patients with AML with MTF2 deficiency (MD-AML) transduced with lentivirus encoding an empty expression vector and treated with daunorubicin remain viable over 48 hours. Right, restoration of MTF2 via lentiviral-induced expression sensitized the MD-AML cells to daunorubicin. **N** (left), Similar results were observed when $CD34^{+}CD38^{-}$ cells isolated from MD-AML patient BM were transduced with control lentivirus treated with cytarabine. Right, MTF2 restoration abolished the chemoresistance observed within 48 hours. **O** and **P,** Viability analysis of UCB $Lin^{-}CD34^{+}$ treated with vehicle control (VC), 2 μmol/L EZH2 inhibitor EPZ005687 (EPZ), or 2 μmol/L of the EZH1/2 inhibitor UNC1999 (UNC) for 72 hours, followed by cotreatment with one of two induction drugs (**O**) daunorubicin (D) or (**P**) cytarabine (C) over 48 hours. **Q** and **R,**Viability analysis of B-AML Lin^{-} $CD34^{+}$ cells that underwent the same treatment regimen as in **O** and **P**. **S–V,** PCNA proliferation marker analysis of (**S** and **T**) UCB Lin $^{-}CD34^{+}$ or (**U** and **V**) B-AML Lin^{-} $CD34^{+}$ cells that underwent the same treatment regimen as in **O** and **P**. PCNA expression in UNC1999 plus either induction drug-treated cells showed significantly increased proliferation over 48 hours. **W–Z,** DNA damage accumulation was assessed by comet assay analysis of (**W** and **X**) UCB $Lin^{-}CD34^{+}$ or (**Y** and **Z**) B-AML Lin^{-} $CD34^{+}$ cells that underwent the same treatment regimen as in **O** and **P**. Cotreatment of UNC1999 plus either induction drug showed the lowest Olive moment representative of DNA damage accumulation over 48 hours. Taken together, these results show that dual loss of both EZH1 and EZH2 is required to confer resistance to standard induction therapy within UCB $Lin^{-}CD34^{+}$ cells and $Lin^{-}CD34^{+}$ leukemic cells. Viable cells were determined by the percentage of Annexin V–negative/7-AAD–negative cells. Representative dot plots are shown in Supplementary Fig. S7A and S7B. Representative comets of each condition are shown in Supplementary Fig. S7C and S7D. All data represent mean ± standard deviation; *, $P < 0.05$; **, $P < 0.005$; ***, $P < 0005$ by two-way ANOVA.

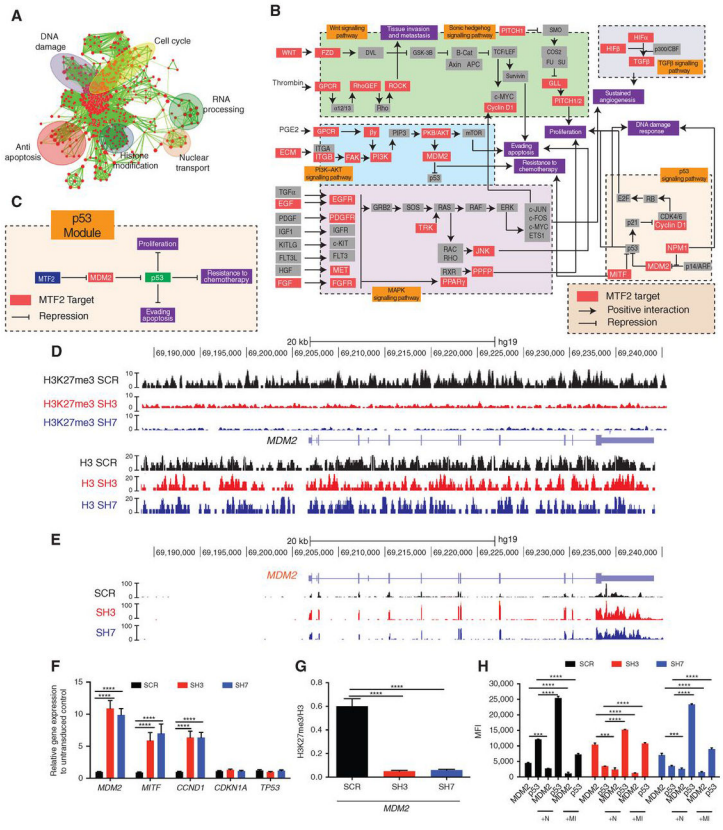

Figure 3.

MTF2 gene regulatory network (GRN) modulates refractory AML via the MDM2/p53 signaling pathway. **A,** Gene ontology enrichment analysis of MTF2 KD UCB Lin^{-}CD34^{+} cells identified genes misregulated in processes such as cell cycle, RNA processing, nuclear transport, antiapoptosis, histone modifications, and DNA damage response (DDR). **B,** MTF2 GRN drafted by the integration of RNA-seq and H3K27me3 ChIP-seq data from hematopoietic progenitors with KEGG pathway analysis uncovered oncogenic pathways that are directly regulated by MTF2-PRC2. **C,**Oncogenic module within the MTF2-PRC2 GRN revealed that MTF2 directly represses MDM2, a direct inhibitor of p53. **D,** Drosophila chromatin spike-in normalized ChIP-seq traces show loss of the repressive H3K27me3 marks at the *MDM2* genomic locus in MTF2 KD UCB Lin^{-}CD34^{+} cells relative to total Histone 3 signal. **E,** RNA-seq traces display increased *MDM2* mRNA levels in MTF2 KD UCB Lin^{-}CD34^{+} cells. **F,** RT-qPCR confirmation of target genes (*MDM2, MITF*, and *CCND1*), nontargets (*CDKN1A* and *TP53*), and (**G**) ChIP-qPCR confirmation of *MDM2* as a target of MTF2 by loss of H3K27me3 following knockdown of MTF2 in UCB Lin^{-}CD34^{+} cells using SH3 and SH7 shRNAs. **H,** Imaging flow cytometry analysis of MDM2 and p53 revealed increased MDM2 and decreased p53 levels within MTF2 shRNA (SH3 or SH7) KD UCB Lin^{-}CD34^{+} cells. Decreased p53 levels within MTF2-deficient UCB Lin^{-}CD34^{+} cells were rescued by treatment with MDM2 inhibitors Nutlin3A (N) or MI-773 (MI). All analyses compared MTF2 KD (SH3 or SH7) with scramble control (SCR) UCB Lin^{-}CD34^{+} cells. All data represent mean ± standard deviation; ***, $P < 0005$; ****, $P < 0.00005$ by two-way ANOVA.

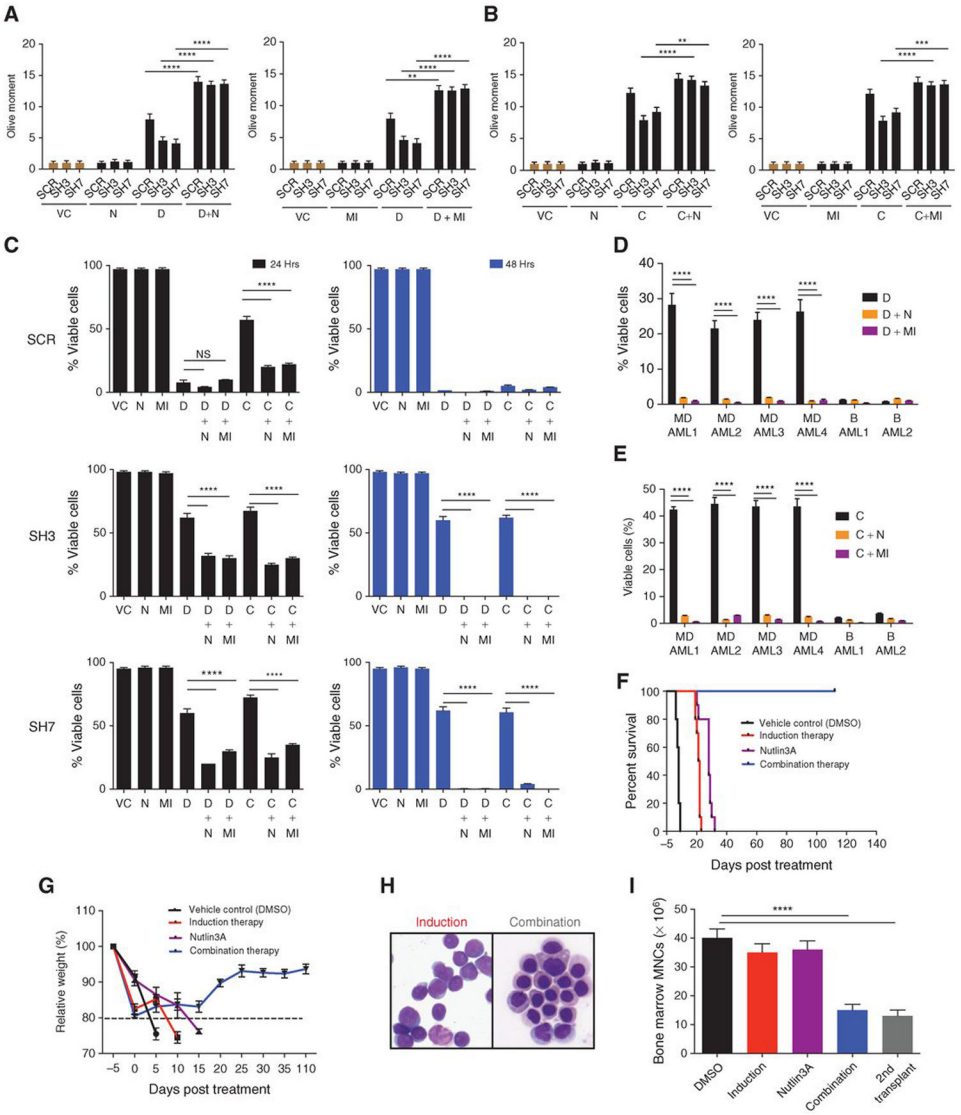

Figure 4.

MDM2 inhibitors sensitize MTF2-deficient hematopoietic progenitors and patient-refractory AML cells to standard treatment of care. **A** and **B,** Alkaline comet assays were performed on control (SCR) and MTF2 KD (SH3, SH7) UCB $Lin^{-}CD34^{+}$ cells treated with vehicle control (VC), (**A**) daunorubicin (D), or (**B**) cytarabine (C) in combination with one of two MDM2 inhibitors, Nutlin3A (N) or MI-773 (MI). **C–E,** Viability analysis to assess chemoresistance posttreatment with induction drugs, MDM2 inhibitors, or both. **C,** MTF2 KD (SH3, SH7) UCB $Lin^{-}CD34^{+}$ cells undergo apoptosis post combination treatment with induction drug plus MDM2 inhibitor, over 48 hours. MTF2-deficient refractory AML cells (MD-AML) showed increased sensitivity to (**D**) daunorubicin and (**E**) cytarabine, when treated in combination with MI-773 (MI) or Nutlin3A (N) for 48 hours comparable to MTF2-basal AML samples (B-AML). Analysis 24 hours after treatment is shown in Supplementary Fig. S23A and S23B. **F,** Kaplan–Meier curve of MD-AML PDX NSG mice treated with either vehicle control, Nutlin3A alone, induction therapy, or combination

therapy (Nutlin3A + induction therapy; $n = 4$ refractory AML samples; $n = 8$ mice per treatment group). **G,** Mouse weight was monitored up to 16 weeks after treatment. Initial weight loss was observed in all conditions, but weight recovery was observed only in mice that underwent combination treatment. **H,** Wright–Giemsa stained cytospins of BM samples from MD-AML PDX mice treated with induction therapy and combination therapy demonstrate a loss of immature blast cells following combination treatment only. **I,** BM mononuclear cell (MNC) counts from MD-AML PDX moribund mice following treatment with either vehicle control (VC), Nutlin3A, or induction therapy and from surviving mice administered combination therapy 16 weeks after treatment and their secondary transplant recipients. A profound decrease in MNCs was observed in the BM of primary mice that received combination therapy and their secondary transplant recipients. Engraftment of secondary transplants is shown in Supplementary Fig. S26. All data represent mean ± standard deviation; *, $P < 0.05$; **, $P < 0.005$; ***, $P < 0005$; $P < 0.00005$ by two-way ANOVA.